Bi-allelic Variants in *METTL5* Cause Autosomal-Recessive Intellectual Disability and Microcephaly

Elodie M. Richard,[1,14] Daniel L. Polla,[2,3,14] Muhammad Zaman Assir,[4,5,6] Minerva Contreras,[7] Mohsin Shahzad,[4,6] Asma A. Khan,[8] Attia Razzaq,[2,8] Javed Akram,[4,6,9] Moazzam N. Tarar,[6] Thomas A. Blanpied,[7] Zubair M. Ahmed,[1] Rami Abou Jamra,[10,11] Dagmar Wieczorek,[12,13] Hans van Bokhoven,[2] Sheikh Riazuddin,[4,6,8,*] and Saima Riazuddin[1,*]

Intellectual disability (ID) is a genetically and clinically heterogeneous disorder, characterized by limited cognitive abilities and impaired adaptive behaviors. In recent years, exome sequencing (ES) has been instrumental in deciphering the genetic etiology of ID. Here, through ES of a large cohort of individuals with ID, we identified two bi-allelic frameshift variants in *METTL5*, c.344_345delGA (p.Arg115Asnfs*19) and c.571_572delAA (p.Lys191Valfs*10), in families of Pakistani and Yemenite origin. Both of these variants were segregating with moderate to severe ID, microcephaly, and various facial dysmorphisms, in an autosomal-recessive fashion. METTL5 is a member of the methyltransferase-like protein family, which encompasses proteins with a seven-beta-strand methyltransferase domain. We found *METTL5* expression in various substructures of rodent and human brains and METTL5 protein to be enriched in the nucleus and synapses of the hippocampal neurons. Functional studies of these truncating variants in transiently transfected orthologous cells and cultured hippocampal rat neurons revealed no effect on the localization of METTL5 but alter its level of expression. Our *in silico* analysis and 3D modeling simulation predict disruption of METTL5 function by both variants. Finally, *mettl5* knockdown in zebrafish resulted in microcephaly, recapitulating the human phenotype. This study provides evidence that biallelic variants in *METTL5* cause ID and microcephaly in humans and highlights the essential role of METTL5 in brain development and neuronal function.

Intellectual disability (ID) is characterized by significant impairment in cognitive ability and adaptive behaviors, with a disease onset generally before adulthood.[1] With a prevalence of 1%–2% worldwide,[2,3] ID is a complex group of disorders that has high phenotypic variability as well as heterogeneous etiology, encompassing genetic and environmental factors.[4] Autosomal-recessive ID (ARID) is estimated to account for more than 50% of genetic causes of ID.[4] The identification of novel ARID genes has gained momentum in recent years through implementation of contemporary high-throughput sequencing technologies (e.g., exome sequencing) and study of large consanguineous families.[5–12] However, these molecular studies highlight extreme genetic heterogeneity with an estimate of more than 2,500 genes associated with various forms of ID.[13]

Here, we illustrate the integration of two large-scale studies, GENCODYS[6] and CARID,[9] and subsequent functional analyses to identify variants that affect function in *METTL5*, segregating with ID, microcephaly, and facial dysmorphisms in two large families of Pakistani and Yemenite origin. Written informed consents were obtained for all individuals involved. This study adhered to the World Health Association Declaration of Helsinki (2013) and was approved by the Institutional Review Board at University of Maryland School of Medicine, Baltimore, USA, Center of Excellence in Molecular Biology (CEMB), University of the Punjab, Lahore, Pakistan, the Institutional Review Board Commissie Mensgebonden Onderzoek Regio Arnhem-Nijmegen, the Netherlands, and an ethical votum for MRNET in Erlangen, Germany. Medical and family history, developmental childhood milestones, anthropometric measurements, and findings of physical examination were collected and detailed clinical phenotypes were described with Human Phenotype Ontology (HPO) terms.[14] Venous blood samples were collected from research participants for DNA extraction.

Family 1 (PKMR43M; Figure 1A; Table 1) was enrolled from Dargai, Malakand Agency in Khyber Pakhtoon Khawa province of Pakistan. There are five individuals presenting with severe ID (HP:0010864), of which two were deceased at the time of assessment. The age of affected

[1]Department of Otorhinolaryngology Head & Neck Surgery, School of Medicine, University of Maryland, Baltimore, MD 21201, USA; [2]Department of Human Genetics, Donders Institute for Brain, Cognition and Behaviour, Radboud university medical center, 6500 HE Nijmegen, the Netherlands; [3]CAPES Foundation, Ministry of Education of Brazil, Brasília DF70040-020, Brazil; [4]Center for Genetic Diseases, Shaheed Zulfiqar Ali Bhutto Medical University, Pakistan Institute of Medical Sciences, Islamabad 44000, Pakistan; [5]Allama Iqbal Medical College, University of Health Sciences, Lahore 54550, Pakistan; [6]Jinnah Burn and Reconstructive Surgery Center, Allama Iqbal Medical College, University of Health Sciences, Lahore 54550, Pakistan; [7]Department of Physiology, School of Medicine, University of Maryland, Baltimore, MD 21201, USA; [8]National Centre of Excellence in Molecular Biology, University of The Punjab, Lahore 53700, Pakistan; [9]University of Health Sciences, Lahore 54000, Pakistan; [10]Institute of Human Genetics, Friedrich-Alexander-Universität Erlangen-Nürnberg, 91054 Erlangen, Germany; [11]Institute of Human Genetics, University Medical Center Leipzig, 04103 Leipzig, Germany; [12]Institut für Humangenetik, Universitätsklinikum Düsseldorf, Heinrich-Heine-Universität, 40225 Düsseldorf, Germany; [13]Institut für Humangenetik, Universitätsklinikum Essen, Universität Duisburg-Essen, 45147 Essen, Germany
[14]These authors contributed equally to this work
*Correspondence: riazuddin@aimrc.org (S.R.), sriazuddin@som.umaryland.edu (S.R.)
https://doi.org/10.1016/j.ajhg.2019.09.007.

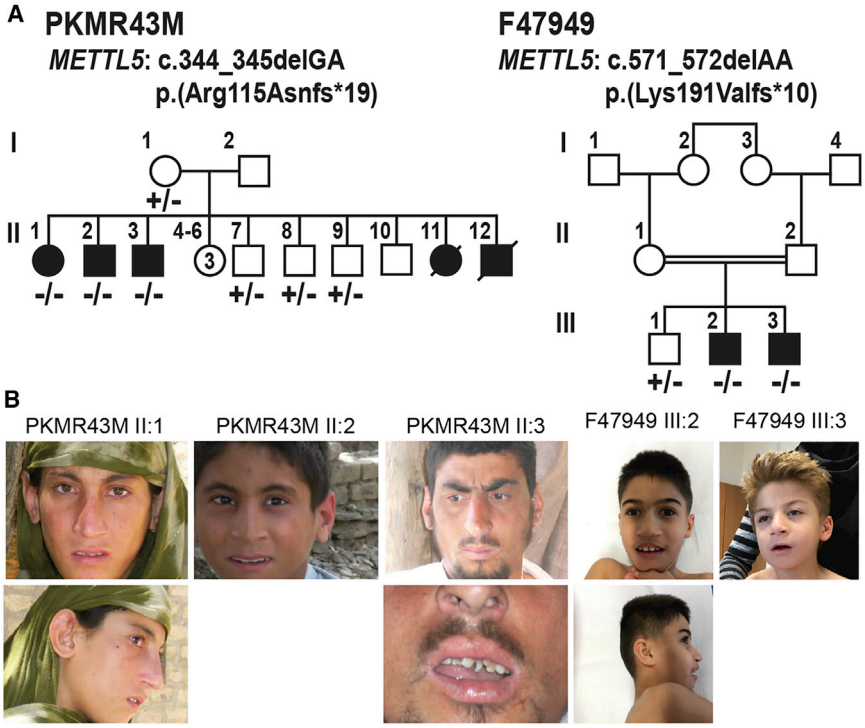

Figure 1. Homozygous Frameshift Variants in *METTL5* Lead to Intellectual Disabilities Associated with Dysmorphic Features

(A) Pedigrees of Pakistani family PKMR43M and Yemenite family F47949 segregating intellectual disabilities and microcephaly due to different frameshift deletions in *METTL5*, c.344_345delGA and c.571_572delAA, respectively. The filled symbols represent affected individuals and a double horizontal line connecting parents represents a consanguineous marriage.

(B) Facial appearance of affected individuals. All affected individuals have microcephaly. Various facial dysmorphisms were reported such as large ear shape (PKMR43M II:1, F47949 III:2), dental anomalies (PKMR43M II:3), and large nose (F47949 III:2).

individuals at the time of evaluation ranged from 14 to 31 years, but the ID was already apparent in early childhood. All three affected individuals had significant delay in childhood milestones including verbal, fine motor, and social skills. There was no history of epilepsy. The apparent behavioral and physical abnormalities noticed in the affected individuals included attention deficit hyperactivity disorder (ADHD) (HP:0007018), aggressive behavior (HP:0000718), microcephaly (HP:0000252), muscular hypotonia (HP:0001252), overhanging nasal tip (HP:0011833), wide nasal base (HP:0012810), and abnormality of dental morphology (HP:0006482) (Figure 1B; Table 1). The affected female had short stature (HP:0004322) and decreased body weight (HP:0004322), i.e., height and weight below 3rd percentile for her age and gender. Evaluation of motor system was unremarkable and gait was normal in all affected individuals with no apparent hearing or vision loss (Table 1). Magnetic resonance imaging (MRI) of the individual II:2 confirmed the measured microcephaly and did not reveal any degeneration of brain tissue (Figure S1).

Family 2 (F47949; Figure 1A; Table 1) had Yemenite origin and was enrolled and evaluated in Germany at the Institutes of Human Genetics in Essen and Düsseldorf. Two affected male individuals were 7 and 12 years old at the time of enrollment and clinical evaluation. Birth history was significant for fetal tachycardia and non-immune hydrops fetalis (HP:0001790) in affected individual III:3, while secundum atrial septal defect (HP:0001684) and pulmonic stenosis (HP:0004415) was observed in affected individual III-2. One affected individual presented severe ID (HP:0010864) and the other one moderate to severe ID (HP:0002342). Both affected individuals had delayed childhood milestones, self-mutilating behavior (HP:0000742), and autism spectrum disorder (HP:0000729). There was no history of epilepsy or motor weakness. Physical examination was significant for microcephaly (HP:0000252), short stature (HP:0004322), low body weight (HP:0004325), wide nasal base (HP:0012810), large nose with broad nasal tip (HP:0000455), low-set and posteriorly rotated ears, and truncal ataxia (HP:0002078) (Figure 1B; Table 1). Overall, the two families presented with a phenotype of ID, speech delay, and microcephaly segregating in an autosomal-recessive inheritance pattern (Figure 1A; Table 1; see Supplemental Note).

Exome sequencing was performed on DNA from one affected individual from each family at Radboudumc, Nijmegen, the Netherlands[6] and at the Institute of Human Genetics, Erlangen, Germany.[9] Among ≥15 variants that passed our initial filtration criteria (see Riazuddin et al.[6] and Reuter et al.[9] for complete description), Sanger sequencing revealed segregation of two novel bi-allelic 2-bp deletions, c.344_345delGA and c.571_572delAA, in *METTL5* (GenBank: NM_014168.2) with the ID phenotype in families PKMR43M and F47949, respectively (Figure 1A). Both variants are predicted to disrupt the reading frame and cause premature truncation (p.Arg115Asnfs*19; p.Lys191Valfs*10) of the encoded METTL5 protein.

METTL5 is a functionally uncharacterized member of the methyltransferase superfamily, which encompasses 33 METTL proteins with a seven-beta-strand methyltransferase domain. By homology with other family members, it is predicted that METTL5 contains an S-adenosyl-L-methionine-dependent DNA methyltransferase domain and a DNA methylase N6 adenine-specific conserved site. In the event that the mRNA harboring c.344_345delGA

Table 1. Clinical Findings of Affected Individuals from Families PKMR43M and F47949

	Family 1, PKMR43M			Family 2, F47949		Family from Hu et al.[11]	
	c.344_345delGA (p.Arg115Asnfs*19)			c.571_572delAA (p.Lys191Valfs*10)		c.182G>A (p.Gly61Asp)	
Individual	**II:1**	**II:2**	**II:3**	**III:3**	**III:2**	**III:3**	**III:5**
Gender	female	male	male	male	male	male	female
Age at evaluation	16 years	14 years	31 years	7 years	12 years	10 years	5 years
Congenital anomalies	no	no	no	fetal tachycardia, hydrops fetalis	ASDII, pulmonic stenosis	not reported	not reported
General Features							
Mental retardation	severe	severe	severe	severe	moderate to severe	severe	severe
Speech delay	yes	yes	yes	yes, no speech	yes, 4–5 word sentences	slurred speech	not reported
Weight	32 kg (−4.9 SD)	50 kg (−0.1 SD)	89 kg (1.9 SD)	16 kg (−3.5 SD)	26 kg (−2.8 SD)	N/A	N/A
Height	152 cm (−1.6 SD)	157 cm (−0.8 SD)	157 cm (−2.7 SD)	114 cm (−2 SD)	135 cm (−2.3 SD)	133 cm (25%ile)	95 cm (3%ile)
Head circumference	51 cm (−3.1 SD)	48 cm (−4.2 SD)	51 cm (−2.8 SD)	46 cm (−5 SD)	48 cm (−4.7 SD)	46 cm (−7 SD)	44 cm(−8 SD)
Head Size	microcephaly	microcephaly	microcephaly	microcephaly	microcephaly	microcephaly	microcephaly
Hypotonia	no	mild	no	no	no	N/A	N/A
Epilepsy	no	no	no	no	no	no	seizure
Spasticity	no	no	no	yes	yes	N/A	N/A
Behavioral problem	ADHD	ADHD, aggressive	ADHD, aggressive	hand biting, autistic	hand biting, autistic	short temper, aggressive	short temper, aggressive
Eyes							
Abnormalities	no	no	no	no	no	strabismus	strabismus
Nose							
Nose shape anomalies	no	broad nasal base, over hanging nasal tip	over hanging nasal tip	large nose with broad tip	large nose with broad tip	narrow nasal base, broad nasal ridge	narrow nasal base, broad nasal ridge
Mouth							
Dental anomalies	no	no	dysplastic teeth	no	no	N/A	N/A
Shape anomalies	no	no	no	no	no	long philtrum and thin upper lip	long philtrum and thin upper lip
Ear							
Ear shape anomalies	large	no	large	low-set and posteriorly rotated	low-set and posteriorly rotated	large	no
Hearing loss	no	no	no	no	no	not reported	not reported
Vestibular deficit	no	no	no	no	no	unbalanced gait	no

ASDII, atrial septal defect type II; ADHD, attention-deficit/hyperactivity disorder

escapes the predicted non-mediated decay[15] *in vivo*, the resulting protein will lack the fully functional S-adenosyl-L-methionine-dependent methyltransferase domain and DNA methylase N6 adenine-specific site, whereas the different predicted domains will remain conserved in METTL5^{L191Vfs*10} (Figure 2A).

We analyzed the expression profile of *METTL5* in the developing and adult human brain (8 pcw to 40 years old), from the RNA-seq data available in the Allen Brain Atlas (see Web Resources). *METTL5* is expressed from very early development (8 pcw) and expression persists through adulthood in multiple sub-structures of the human brain, including the cerebellar cortex, hippocampus, and striatum (Table S1). To characterize the cellular localization of METTL5, we used commercially available polyclonal antibody (NBP1-56640, RRID: AB_11039697,

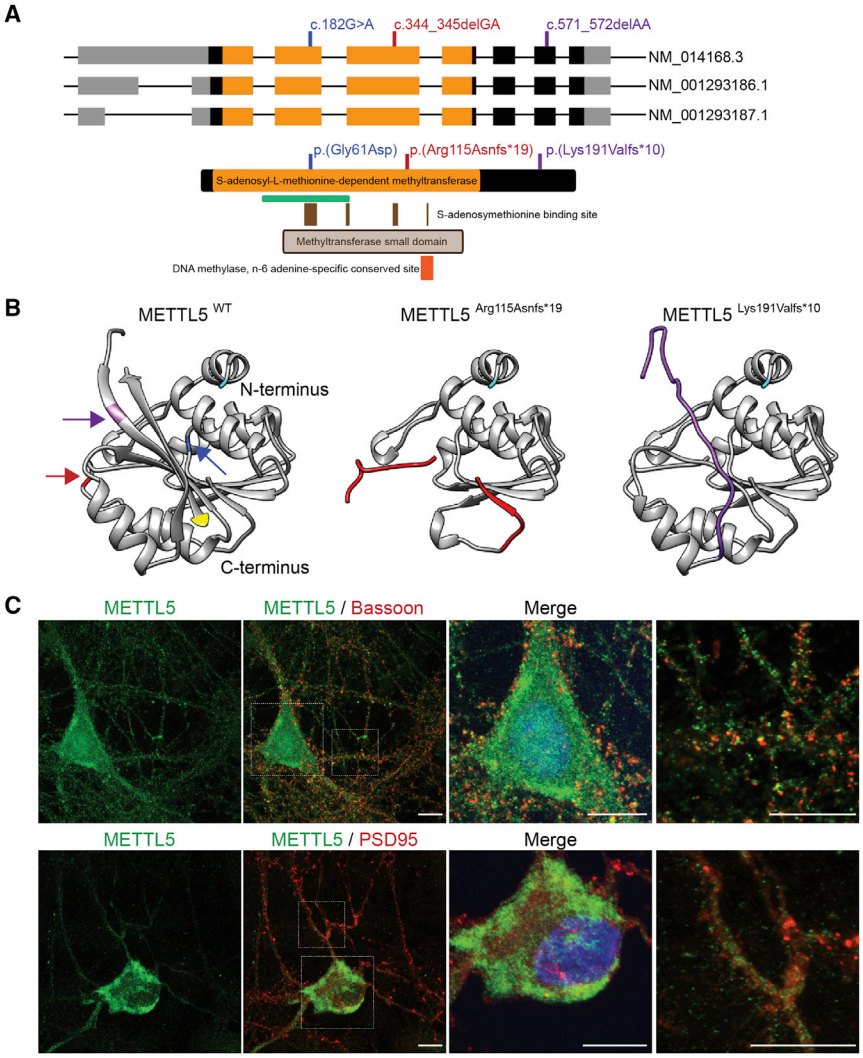

Figure 2. Frameshift Variants in *METTL5* Impact the Predicted Domains and Conformation of the Protein, Ubiquitously Expressed in the Brain

(A) Alternative splicing leads to three isoforms of human METTL5. Non-coding segments and coding regions of exons are denoted by gray and black boxes, respectively. Regions coding for the S-adenosyl-L-methionine-dependent-methyltransferase domain are colored in orange. Variants analyzed in this study are depicted in red (PKMR43M), purple (F47949), and blue.[11] The numbering of the position of variants c.182G>A (p.Gly61Asp), c.344_345delGA (p.Arg115Asnfs*19), and c.571_572delAA (p.Lys191Valfs*10) is based on accession number GenBank: NM_014167.2. The three isoforms lead to a unique protein, predicted to contain an S-adenosyl-L-methionine-dependent-methyltransferase (orange, amino acids 12–161), a methyltransferase small domain (brown box, amino acids 46–146), S-adenosylmethionine binding sites (dark brown box, amino acids 58L, 59G, 60C, 61G, 62C, 63G, 64V, 81D, 82I, 107C, 108D, 109V, 126V), and a DNA-methylase n-6-adenine-specific conserved site (red box, amino acids 123–129). The localization of the peptide used to produce the METTL5 antibody described in the following analysis is shown as a green bar (Novus Biologicals Cat# NBP1-56640, RRID:AB_11039697, amino acids 35–83).

(B) Protein modeling of the WT and the two novel mutant proteins, using PHYRE2 software,[16] shows that the overall conformation of the protein is not affected by the different disease-causing variants. However, due to early termination codon, 2 α helix and 2 β sheet are missing in $METTL5^{R115Nfs*19}$ and 2 β sheet are missing in $METTL5^{L191Vfs*10}$. The red and purple arrows represent the site of truncation in variant p.Arg115Asnfs*19 and p.Lys191Valfs*10, respectively, and the blue arrow highlights the amino acid at position 61. Cyan, N terminus of the protein; yellow, C terminus of the protein.

(C) Representative immunofluorescent labeling images of endogenous METTL5 (green) highlight the partial co-localization of the WT protein with pre-synaptic (Bassoon, Enzo Life Sciences Cat# SAP7F407, RRID:AB_2313990, red) and post-synaptic (PSD95, UC Davis/NIH NeuroMab Facility Cat# 75-028, RRID:AB_2292909, red) markers in rat hippocampal neurons in culture. All images are projection of confocal optical sections stack. Scale bars: 10 μm.

Novus Biologicals) (Figure S2) and performed immunostaining and confocal imaging on postnatal (P) day 30 mouse brain. Similar to humans, we found low but ubiquitous expression in the mouse brain (Figure S3). Immunolabeling of cultured rat hippocampal neurons showed an enrichment of METTL5 in the soma and the nucleus as well as in the pre- and post-synaptic regions (Figure 2D). Taken together with the domain structures, these data suggest that METTL5 might have a global epigenetic regulatory role in the brain as well as a synapse-dependent role. Several publications highlighted the importance of synapse-autonomous regulatory mechanisms,[17,18] including regulation involving METTL proteins.[19]

To evaluate the functional impact of the ID-associated variants on METTL5 protein structure and function, we first performed molecular modeling using PHYRE2[16] and Chimera[20] programs (Figure 2C). As anticipated, both frameshift variants (c.344_345delGA and c.571_572delAA) are predicted to have significant impact on the protein secondary structure and remove the evolutionary conserved two α helix and/or β sheets from the C-terminal region.

To functionally validate the *in silico* predictions, we next investigated the impact of the variants on the stability and/or targeting of METTL5 in heterologous cells. We included in our study another candidate missense variant (c.182G>A [p.Gly61Asp]) (Figures 2A and 2B) that has been recently reported in an Iranian family with two affected individuals. While clinical features were similar to the phenotypes (Table 1) found in our two families, including severe ID, microcephaly, short temper, aggressive behavior, and various facial dysmorphisms,[11] no

functional studies were performed to determine the pathogenicity of the p.Gly61Asp variant on the encoded METTL5.

For these studies, full-length *METTL5* was amplified from a human liver tissue cDNA library (TakaraBio) and was inserted in pCMV-Myc and peGFP-C2 vectors (TakaraBio). The constructs harboring ID-associated variants ($METTL5^{G61D}$; $METTL5^{R115Nfs*19}$; $METTL5^{L191Vfs*10}$) were prepared through site-directed mutagenesis (Agilent Technologies) using the wild-type construct ($METTL5^{WT}$) as a template. All constructs sequences were validated by Sanger sequencing (primers sequences are available upon request). When transiently expressed in COS7 cells, both Myc- and GFP-tagged $METTL5^{WT}$ as well as mutant proteins were found in the cytoplasm and in slightly higher amounts in the nucleus (Figures 3A and S4A). Similarly, when transfected in cultured rat hippocampal neurons, wild-type and mutant METTL5-GFP tagged proteins were observed in the nucleus, as well as in the neuronal dendrites (Figure S5).

In COS7 cells, no apparent difference in the levels and localization of $METTL5^{G61D}$ protein was observed, when compared with wild-type METTL5 (Figure 3B). In contrast, the levels of $METTL5^{R115Nfs*19}$ and $METTL5^{L191Vfs*10}$ were significantly reduced as compared to wild-type METTL5 (Figure 3B). Western blot analyses using transiently transfected HEK293T cells further confirmed that both truncating variants significantly (**$p < 0.01$, ***$p < 0.001$) affected the stability of the mutant METTL5 protein (Figures 3C, 3D, and S4). To determine whether the observed decrease in protein expression is due to protein instability, we challenged the stability of Myc-tagged proteins. At 48 h post transfection, cells were treated for 4 h with either MG132 (50 μM, proteasome inhibitor, Sigma-Aldrich) or CHX (cyclohexamide, 0.1 mM, synthesis blocker, Sigma-Aldrich). Post-MG132-treatment western blot analysis revealed a dramatic increase in the levels of truncated proteins while post-CHX treatment did not highlight any remarkable difference between the WT and the mutant proteins, which suggest that c.344_345delGA and c.571_572delAA variants significantly reduce the stability of the corresponding proteins (Figure 3E).

We next investigated the function of Mettl5 in the developing brain and neurons in zebrafish, which express the orthologous *mettl5* gene (GenBank: NM_001005949.1) throughout development (Figure 4A).[22] Using specific translation blocking morpholino (MO) (5′-GCTCTCCAGC TCTTTCAGCTTCATT-3′; 2 ng) and splice site (exon 3) targeting MO (5′-GGTTAGTGAGTTTTCTTACCCTGGT-3′; 5 ng), we knocked down *mettl5* in embryos of NeuroD-eGFP transgenic zebrafish strain.[23] At 72 h post-fertilization (hpf) *mettl5* morphants had reduced head size, mimicking the human microcephaly, and curved tails, while the control morpholino (5′- CCTCTTACCTCAGTTA CAATTTATA-3′)-injected embryos had normal growth (Figures 4B, 4C, and S6). To rule out MO toxicity, we used various dilutions and also blocked the p53 pathway via co-injection of a *p53*-targeting MO.[24] The phenotype of the co-injected embryos was identical to that of those injected with the *Mettl5* ATG blocker or splice-targeting MO alone. Thus, morphant developmental deficits appear to be specific to the knockdown of *mettl5* expression. Next, we further examined the brain structure in *mettl5* morphants and controls embryos. Although no statistically significant difference in hindbrain size was observed, both the forebrain and the midbrain were adversely altered with a 24%–26% and 16%–23% size reduction, respectively ($p < 0.0001$), which further confirms the essential role of *mettl5* in brain development.

Even though the precise function of METTL5 is currently uncharacterized, our study highlights its essential role in human and zebrafish brain development and cognitive function. In this study, we have identified two bi-allelic frameshift variants: c.344_345delGA and c.571_572delAA. Despite a low pLI score for *METTL5* (pLi = 0), no loss-of-function variants in a homozygous state was found in the gnomAD database, indicating the in-tolerance to bi-allelic truncating variants. Our functional analyses revealed that both c.344_345delGA and c.571_572delAA variants drastically impact the expression and the conformation of the protein (Figures 2 and3), and thus taken together with the genetic and *in silico* analysis, both these variants can be classified as "pathogenic" according to the ACMG/AMP guidelines[25] (Table S2). The candidate missense variant p.Gly61Asp reported previously,[11] replacing highly evolutionary conserved amino acid (Figure S7), is predicted to be pathogenic by several *in silico* algorithms (Table S3). However, our 3D modeling (Figure S7) as well as expression and localization studies (Figure 3) failed to demonstrate a functional impact on the encoded protein, and thus classified here as "variant of uncertain significance" (Table S2).

In humans, variants in METTL proteins have been associated with various disorders, such as sclerosis (METTL1[26] [MIM: 404466]), liver cancer (METTL3[27] [MIM: 612472]), breast cancer (METTL3,[28] METTL6[29]), colon cancer (METTL8 [MIM: 609525] and METTL16[30]), pancreatic cancer (METTL13[31] [MIM: 617987]), otoprotection/hearing loss (MIM: 605429) (METTL13[32]), and osteoporosis (METTL21C[33] [MIM: 615259]). Furthermore, variants in other methyltransferase-like genes associated with ID have been reported previously.[34–37] For instance, truncating alleles of *METTL23* (MIM: 615262) have been identified in families with mild non-syndromic ARID or cognitive dysfunction with mild dysmorphic features (MIM: 615942). Similarly, micro-duplications (351 kb and 432 kb genomic region), both containing *METTL4* among other genes, were associated with ID and mild dysmorphic features.[36,37] In addition to these METTL proteins, various methyltransferases, including histone methyltransferases (*EHMT1*[38] [MIM: 607001], *KMT2A*[39] [MIM: 159555]), DNA methyltransferase (*DNMT3A*[40] [MIM: 602769]), tRNA (*TRMT1*[41] [MIM: 611669], *NSUN2*[42,43] [MIM: 610916]), and rRNA methyltransferases (*FTSJ1*[44] [MIM:

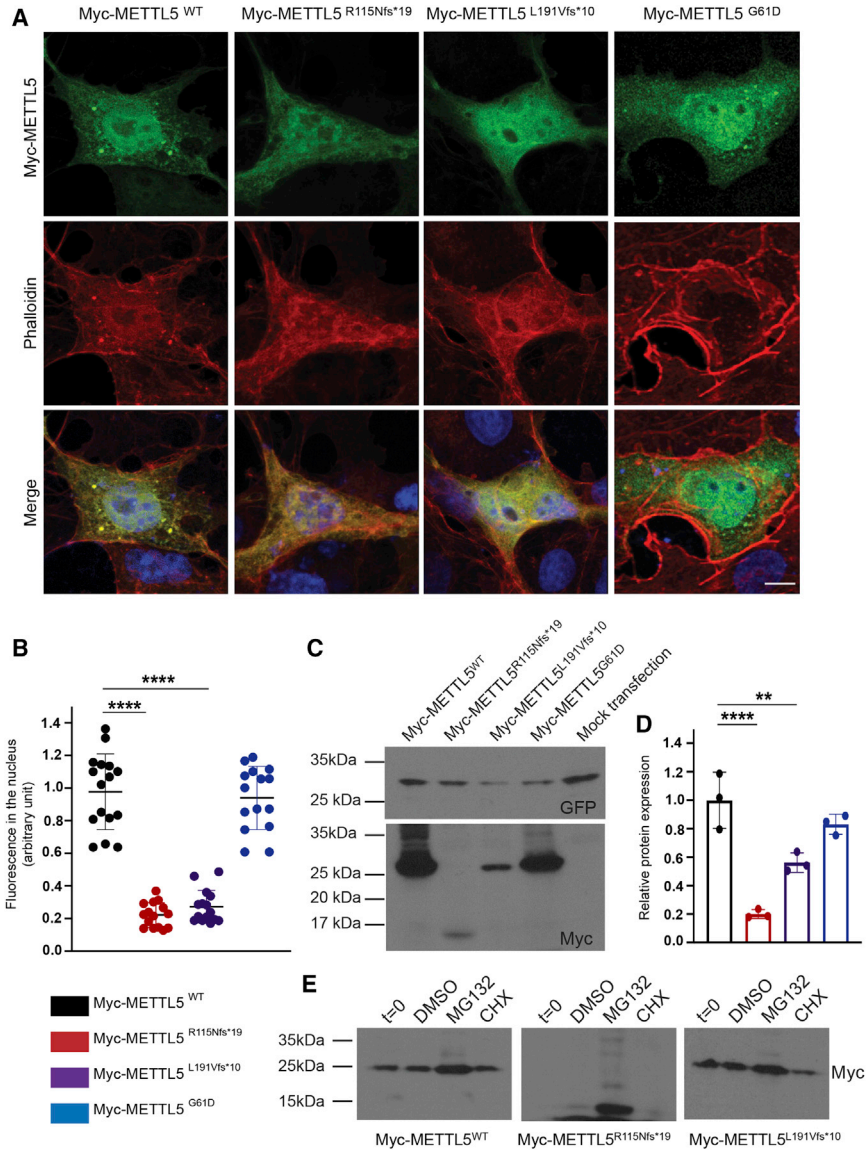

Figure 3. Disease-Causing Variants Affect the Stability of METTL5

(A) Immunolabeling of Myc-METTL5 fusion proteins for WT and the three variants associated with ID, after transfection in COS7 cells. The subcellular localization shows that METTL5 (green) accumulates in the nucleus (blue) and forms aggregates in the cytoplasm. The two frameshift variants as well as the missense variant do not seem to affect this localization. All images are projection of confocal optical sections stack. Scale bar: 10 μm.

(B) Quantification of the signal intensity for METTL5 in the nucleus in the different conditions show that only the truncating variants affect the level of expression of the protein. COS7 cells were co-transfected with peGFP empty vector and the different pCMV-Myc-METTL5 constructs. The intensity of the METTL5 and GFP signals in the nucleus were measured using ImageJ software and averaged from five areas per nucleus. METTL5 signal was normalized against GFP signal, minimizing the effect of transfection efficiency among cells and experiments (one-way ANOVA analysis followed by a Bonferroni post hoc test, ****$p < 0.0001$).

(C and D) Western blot on transfected HEK293T cells with Myc-METTL5 WT or mutant constructs reveals that both frameshift variants decrease the stability of the mutant proteins, but the missense variant does not.

(C) Representative image of western blot assay. An antibody against Myc (Covance Research Products Inc., Cat# MMS-164P-100, RRID:AB_291335) was used to analyze Myc-METTL5 signal. GFP signal was used as a transfection control.

(D) Quantification of the signal intensity for Myc and GFP was measured using ImageJ software. Myc signal intensity was normalized against the GFP signal intensity (one-way ANOVA analysis followed by a Bonferroni post hoc test, **$p < 0.01$, ****$p < 0.0001$).

(E) Representative image of western blot assay. 48 h after transfection, cells were collected ($t = 0$) to assess initial expression level of the protein. Remaining cells were treated either with vehicle (0.5% DMSO), MG132 (50 μM), or cyclohexamide (CHX, 0.1 mM) for 4 h. Mutant METTL5 bands intensity increases drastically after treatment with MG132, while the cyclohexamide treatment does not alter differently WT and mutant proteins, suggesting that the disease-causing variants affect the stability of the protein rather than the mRNAs.

300499]), have been implicated in ID, highlighting the importance of methyltransferases in the brain development and cognitive functions.

A growing body of evidence shows that methyltransferases and other epigenetic regulators play an important role in neurodevelopment and/or neuroplasticity.[45,46] The presence of putative DNA methylase N^6 adenine-specific conserved site as well as the accumulation of METTL5 in the nucleus tend to suggest an important role of METTL5 as an epigenetic regulator. *In silico* and homology analyses predicted METTL5 interaction with DNA; however, there is only experimental evidence showing that it interacts with RNA.[47] N^6-adenine RNA methylation has been implicated in the regulation of gene expression, translation efficiency, mRNA stability,[48] as well as in neuropsychiatric disorders,[49] although the mechanism and impact are not fully understood yet.[50–52] Among others, METTL3 and METTL14 (MIM: 616504) are of particular interest as they belong to the METTL family and form a complex which is important for N^6-adenine RNA methylation.[53] A recent study, using *Mettl14* transgenic mice, showed that *Mettl14* regulates the size of the brain and more particularly the size of the cerebral cortex, via altered histone modifications.[54] Knocking out *Mettl14* specifically in the neural stem cells leads to microcephaly.[54] Similarly, the ablation of *Mettl3* in mice leads

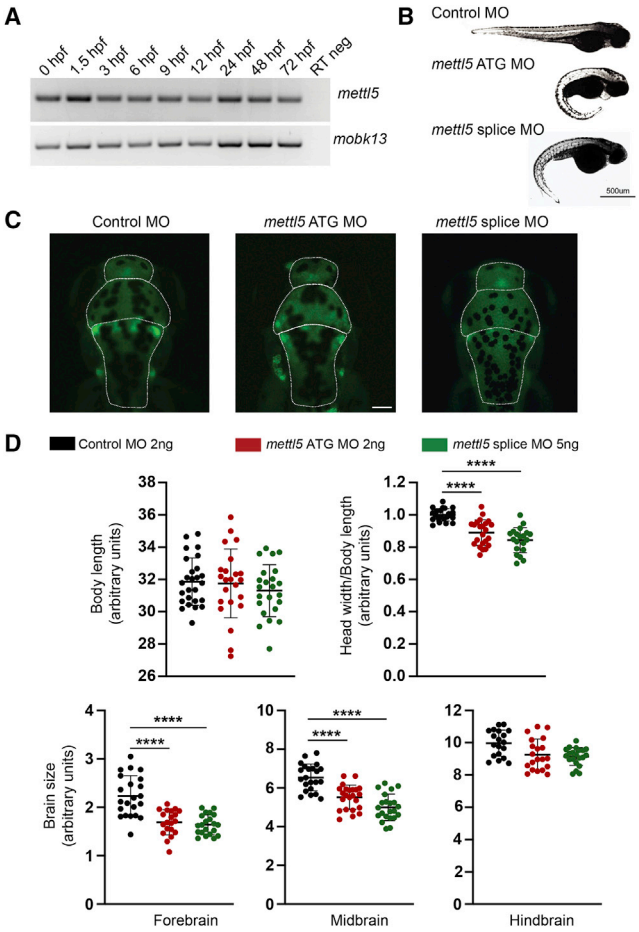

Figure 4. *mettl5* Knock-down in zebrafish Reproduces the Microcephaly Phenotype

(A) *mettl5* is expressed as early as 20 min after fertilization in zebrafish embryos. *mobk13* was used as a loading control. Hpf, hours post fertilization.

(B) Representative images of dorsal view of zebrafish morphology from control, ATG blocker *mettl5* MO, and splice-targeting *mettl5* MO, injected larvae, at 72 hpf. Scale bar: 500 μm.

(C) Representative top images of injected zebrafish's brain, at 72 hpf. Brain area were measured according to the white dotted line. Scale bar: 10 μm.

(D) Zebrafish were imaged from a dorsal and lateral view, at 72 hpf. The total body length as well as the brain maximum width were measured using ImageJ software. The brain width/body length ratio was calculated and normalized against the mean for the fish injected with the Control MO and defined as the "microcephaly index," as previously described.[21] The larvae injected with the *mettl5* ATG MO and splice-targeting MO show a significant microcephaly phenotype compared to the fish injected with the control MO (n = 20/condition, data are represented as the mean ± SD, one-way ANOVA analysis followed by a Bonferroni post hoc test, ****$p < 0.0001$).

(E) Each brain area was measured using ImageJ software and normalized against the mean for the Control MO-injected fish (n = 20/condition, data are represented as the mean ± SD, one-way ANOVA analysis followed by a Bonferroni post hoc test, **** $p < 0.0001$).

to developmental defects associated with depletion of m6A and dramatic change in the expression of apoptosis and cerebellum development-related genes.[55] In addition to their roles in the regulation of brain development, both *Mettl3* and *Mettl14* are key molecules that can alter learning abilities.[56,57] METTL3-METTL14 complex is one of the main components, but it does not account for all the N^6-methyladenosine (m^6A) modifications. The identification of METTL16, another methyltransferase-like protein, as a new m^6A methyltransferase[58] suggests that other methyltransferase-like family members like METTL5 may also carry m^6A methyltransferase activity.

In summary, *METTL5* variants underlie autosomal-recessive ID with microcephaly in humans. *METTL5* is expressed in the developing and aging brain, accumulates in the nucleus and the synapses of neurons, and shares several domains structure with other m^6A modifiers. Therefore, we speculate that human METTL5 participates in the epigenetic regulation of DNA/RNA in the neurons. Our studies reveal that, as in humans, zebrafish Mettl5 is critical for proper brain development and possibly neuronal function.

Supplemental Data

Supplemental Data can be found online at https://doi.org/10.1016/j.ajhg.2019.09.007.

Acknowledgments

We are very thankful to the affected individuals and their families who have participated to this study. We would like to thank Dr. Zaghloul for generously sharing the NeuroD-eGFP zebrafish line with us. We would like to thank Muhammad A. Usmani and Drs. R. Yousaf, S. Yousaf, and A.P.J. Giese for their technical assistance. Confocal images were acquired thanks to the University of Maryland, School of Medicine, CIBR Confocal microscopy core facility and Department of Physiology (Baltimore, Maryland, USA).

This work was supported by NIH R01NS107428 (to Saima Riazuddin), the EU FP7 Large-Scale Integrating Project Genetic and Epigenetic Networks in Cognitive Dysfunction (241995) (to H.v.B.), the DFG (AB 3939 / 2-2) (to R.A.J.), and NRPU Projects from Higher Education commission of Pakistan (to M.S. and J.A.). D.L.P. is recipient of a CAPES Fellowship (99999.013311/2013-01).

Declaration of Interests

The authors declare no competing interests.

Received: April 26, 2019
Accepted: September 4, 2019
Published: September 26, 2019

Web Resources

Allen Brain Atlas, https://portal.brain-map.org/
CADD, https://cadd.gs.washington.edu/
ClinVar, https://www.ncbi.nlm.nih.gov/clinvar/variation/689363/; https://www.ncbi.nlm.nih.gov/clinvar/variation/689379/
ExAC Browser, http://exac.broadinstitute.org/
GenBank, https://www.ncbi.nlm.nih.gov/genbank/
gnomAD Browser, https://gnomad.broadinstitute.org/
InterPro, https://www.ebi.ac.uk/interpro/
MutationTaster, http://www.mutationtaster.org/

OMIM, https://www.omim.org/
PolyPhen-2, http://genetics.bwh.harvard.edu/pph2/
PROVEAN, http://provean.jcvi.org
RRID, https://scicrunch.org/resources

Reference

1. Schalock, R.L., Luckasson, R.A., Shogren, K.A., Borthwick-Duffy, S., Bradley, V., Buntinx, W.H., Coulter, D.L., Craig, E.M., Gomez, S.C., Lachapelle, Y., et al. (2007). The renaming of mental retardation: understanding the change to the term intellectual disability. Intellect. Dev. Disabil. *45*, 116–124.
2. Maulik, P.K., Mascarenhas, M.N., Mathers, C.D., Dua, T., and Saxena, S. (2011). Prevalence of intellectual disability: a meta-analysis of population-based studies. Res. Dev. Disabil. *32*, 419–436.
3. McKenzie, K., and Murray, A.L. (2015). Evaluating the use of the Child and Adolescent Intellectual Disability Screening Questionnaire (CAIDS-Q) to estimate IQ in children with low intellectual ability. Res. Dev. Disabil. *37*, 31–36.
4. Vissers, L.E., Gilissen, C., and Veltman, J.A. (2016). Genetic studies in intellectual disability and related disorders. Nat. Rev. Genet. *17*, 9–18.
5. Harripaul, R., Noor, A., Ayub, M., and Vincent, J.B. (2017). The Use of Next-Generation Sequencing for Research and Diagnostics for Intellectual Disability. Cold Spring Harb. Perspect. Med. *7*, 7.
6. Riazuddin, S., Hussain, M., Razzaq, A., Iqbal, Z., Shahzad, M., Polla, D.L., Song, Y., van Beusekom, E., Khan, A.A., Tomas-Roca, L., et al.; UK10K (2017). Exome sequencing of Pakistani consanguineous families identifies 30 novel candidate genes for recessive intellectual disability. Mol. Psychiatry *22*, 1604–1614.
7. Najmabadi, H., Hu, H., Garshasbi, M., Zemojtel, T., Abedini, S.S., Chen, W., Hosseini, M., Behjati, F., Haas, S., Jamali, P., et al. (2011). Deep sequencing reveals 50 novel genes for recessive cognitive disorders. Nature *478*, 57–63.
8. Anazi, S., Maddirevula, S., Faqeih, E., Alsedairy, H., Alzahrani, F., Shamseldin, H.E., Patel, N., Hashem, M., Ibrahim, N., Abdulwahab, F., et al. (2017). Clinical genomics expands the morbid genome of intellectual disability and offers a high diagnostic yield. Mol. Psychiatry *22*, 615–624.
9. Reuter, M.S., Tawamie, H., Buchert, R., Hosny Gebril, O., Froukh, T., Thiel, C., Uebe, S., Ekici, A.B., Krumbiegel, M., Zweier, C., et al. (2017). Diagnostic Yield and Novel Candidate Genes by Exome Sequencing in 152 Consanguineous Families With Neurodevelopmental Disorders. JAMA Psychiatry *74*, 293–299.
10. Trujillano, D., Bertoli-Avella, A.M., Kumar Kandaswamy, K., Weiss, M.E., Köster, J., Marais, A., Paknia, O., Schröder, R., Garcia-Aznar, J.M., Werber, M., et al. (2017). Clinical exome sequencing: results from 2819 samples reflecting 1000 families. Eur. J. Hum. Genet. *25*, 176–182.
11. Hu, H., Kahrizi, K., Musante, L., Fattahi, Z., Herwig, R., Hosseini, M., Oppitz, C., Abedini, S.S., Suckow, V., Larti, F., et al. (2019). Genetics of intellectual disability in consanguineous families. Mol. Psychiatry *24*, 1027–1039.
12. Harripaul, R., Vasli, N., Mikhailov, A., Rafiq, M.A., Mittal, K., Windpassinger, C., Sheikh, T.I., Noor, A., Mahmood, H., Downey, S., et al. (2018). Mapping autosomal recessive intellectual disability: combined microarray and exome sequencing identifies 26 novel candidate genes in 192 consanguineous families. Mol. Psychiatry *23*, 973–984.
13. Musante, L., and Ropers, H.H. (2014). Genetics of recessive cognitive disorders. Trends Genet. *30*, 32–39.
14. Robinson, P.N., Köhler, S., Bauer, S., Seelow, D., Horn, D., and Mundlos, S. (2008). The Human Phenotype Ontology: a tool for annotating and analyzing human hereditary disease. Am. J. Hum. Genet. *83*, 610–615.
15. Lewis, B.P., Green, R.E., and Brenner, S.E. (2003). Evidence for the widespread coupling of alternative splicing and nonsense-mediated mRNA decay in humans. Proc. Natl. Acad. Sci. USA *100*, 189–192.
16. Kelley, L.A., Mezulis, S., Yates, C.M., Wass, M.N., and Sternberg, M.J. (2015). The Phyre2 web portal for protein modeling, prediction and analysis. Nat. Protoc. *10*, 845–858.
17. Sutton, M.A., and Schuman, E.M. (2006). Dendritic protein synthesis, synaptic plasticity, and memory. Cell *127*, 49–58.
18. Kelleher, R.J., 3rd, Govindarajan, A., and Tonegawa, S. (2004). Translational regulatory mechanisms in persistent forms of synaptic plasticity. Neuron *44*, 59–73.
19. Merkurjev, D., Hong, W.T., Iida, K., Oomoto, I., Goldie, B.J., Yamaguti, H., Ohara, T., Kawaguchi, S.Y., Hirano, T., Martin, K.C., et al. (2018). Synaptic N^6-methyladenosine (m^6A) epitranscriptome reveals functional partitioning of localized transcripts. Nat. Neurosci. *21*, 1004–1014.
20. Goddard, T.D., Huang, C.C., Meng, E.C., Pettersen, E.F., Couch, G.S., Morris, J.H., and Ferrin, T.E. (2018). UCSF ChimeraX: Meeting modern challenges in visualization and analysis. Protein Sci. *27*, 14–25.
21. Jobst-Schwan, T., Schmidt, J.M., Schneider, R., Hoogstraten, C.A., Ullmann, J.F.P., Schapiro, D., Majmundar, A.J., Kolb, A., Eddy, K., Shril, S., et al. (2018). Acute multi-sgRNA knockdown of KEOPS complex genes reproduces the microcephaly phenotype of the stable knockout zebrafish model. PLoS ONE *13*, e0191503.
22. Thisse, B., Heyer, V., Lux, A., Alunni, V., Degrave, A., Seiliez, I., Kirchner, J., Parkhill, J.P., and Thisse, C. (2004). Spatial and temporal expression of the zebrafish genome by large-scale in situ hybridization screening. Methods Cell Biol. *77*, 505–519.
23. Obholzer, N., Wolfson, S., Trapani, J.G., Mo, W., Nechiporuk, A., Busch-Nentwich, E., Seiler, C., Sidi, S., Söllner, C., Duncan, R.N., et al. (2008). Vesicular glutamate transporter 3 is required for synaptic transmission in zebrafish hair cells. J. Neurosci. *28*, 2110–2118.
24. Langheinrich, U., Hennen, E., Stott, G., and Vacun, G. (2002). Zebrafish as a model organism for the identification and characterization of drugs and genes affecting p53 signaling. Curr. Biol. *12*, 2023–2028.
25. Richards, S., Aziz, N., Bale, S., Bick, D., Das, S., Gastier-Foster, J., Grody, W.W., Hegde, M., Lyon, E., Spector, E., et al.; ACMG Laboratory Quality Assurance Committee (2015). Standards and guidelines for the interpretation of sequence variants: a joint consensus recommendation of the American College of Medical Genetics and Genomics and the Association for Molecular Pathology. Genet. Med. *17*, 405–424.
26. Alcina, A., Fedetz, M., Fernández, O., Saiz, A., Izquierdo, G., Lucas, M., Leyva, L., García-León, J.A., Abad-Grau, Mdel.M., Alloza, I., et al. (2013). Identification of a functional variant in the KIF5A-CYP27B1-METTL1-FAM119B locus associated with multiple sclerosis. J. Med. Genet. *50*, 25–33.
27. Chen, M., Wei, L., Law, C.T., Tsang, F.H., Shen, J., Cheng, C.L., Tsang, L.H., Ho, D.W., Chiu, D.K., Lee, J.M., et al. (2018). RNA N6-methyladenosine methyltransferase-like 3 promotes liver

cancer progression through YTHDF2-dependent posttranscriptional silencing of SOCS2. Hepatology *67*, 2254–2270.
28. Cai, X., Wang, X., Cao, C., Gao, Y., Zhang, S., Yang, Z., Liu, Y., Zhang, X., Zhang, W., and Ye, L. (2018). HBXIP-elevated methyltransferase METTL3 promotes the progression of breast cancer via inhibiting tumor suppressor let-7g. Cancer Lett. *415*, 11–19.
29. Gatza, M.L., Silva, G.O., Parker, J.S., Fan, C., and Perou, C.M. (2014). An integrated genomics approach identifies drivers of proliferation in luminal-subtype human breast cancer. Nat. Genet. *46*, 1051–1059.
30. Yeon, S.Y., Jo, Y.S., Choi, E.J., Kim, M.S., Yoo, N.J., and Lee, S.H. (2018). Frameshift Mutations in Repeat Sequences of ANK3, HACD4, TCP10L, TP53BP1, MFN1, LCMT2, RNMT, TRMT6, METTL8 and METTL16 Genes in Colon Cancers. Pathol. Oncol. Res. *24*, 617–622.
31. Liu, S., Hausmann, S., Carlson, S.M., Fuentes, M.E., Francis, J.W., Pillai, R., Lofgren, S.M., Hulea, L., Tandoc, K., Lu, J., et al. (2019). METTL13 Methylation of eEF1A Increases Translational Output to Promote Tumorigenesis. Cell *176*, 491–504.e21.
32. Yousaf, R., Ahmed, Z.M., Giese, A.P., Morell, R.J., Lagziel, A., Dabdoub, A., Wilcox, E.R., Riazuddin, S., Friedman, T.B., and Riazuddin, S. (2018). Modifier variant of METTL13 suppresses human GAB1-associated profound deafness. J. Clin. Invest. *128*, 1509–1522.
33. Huang, J., Hsu, Y.H., Mo, C., Abreu, E., Kiel, D.P., Bonewald, L.F., Brotto, M., and Karasik, D. (2014). METTL21C is a potential pleiotropic gene for osteoporosis and sarcopenia acting through the modulation of the NF-κB signaling pathway. J. Bone Miner. Res. *29*, 1531–1540.
34. Bernkopf, M., Webersinke, G., Tongsook, C., Koyani, C.N., Rafiq, M.A., Ayaz, M., Müller, D., Enzinger, C., Aslam, M., Naeem, F., et al. (2014). Disruption of the methyltransferase-like 23 gene METTL23 causes mild autosomal recessive intellectual disability. Hum. Mol. Genet. *23*, 4015–4023.
35. Reiff, R.E., Ali, B.R., Baron, B., Yu, T.W., Ben-Salem, S., Coulter, M.E., Schubert, C.R., Hill, R.S., Akawi, N.A., Al-Younes, B., et al. (2014). METTL23, a transcriptional partner of GABPA, is essential for human cognition. Hum. Mol. Genet. *23*, 3456–3466.
36. Kashevarova, A.A., Nazarenko, L.P., Skryabin, N.A., Salyukova, O.A., Chechetkina, N.N., Tolmacheva, E.N., Sazhenova, E.A., Magini, P., Graziano, C., Romeo, G., et al. (2014). Array CGH analysis of a cohort of Russian patients with intellectual disability. Gene *536*, 145–150.
37. Kashevarova, A.A., Nazarenko, L.P., Skryabin, N.A., Nikitina, T.V., Vasilyev, S.A., Tolmacheva, E.N., Lopatkina, M.E., Salyukova, O.A., Chechetkina, N.N., Vorotelyak, E.A., et al. (2018). A mosaic intragenic microduplication of LAMA1 and a constitutional 18p11.32 microduplication in a patient with keratosis pilaris and intellectual disability. Am. J. Med. Genet. A. *176*, 2395–2403.
38. Kleefstra, T., Brunner, H.G., Amiel, J., Oudakker, A.R., Nillesen, W.M., Magee, A., Geneviève, D., Cormier-Daire, V., van Esch, H., Fryns, J.P., et al. (2006). Loss-of-function mutations in euchromatin histone methyl transferase 1 (EHMT1) cause the 9q34 subtelomeric deletion syndrome. Am. J. Hum. Genet. *79*, 370–377.
39. Lebrun, N., Giurgea, I., Goldenberg, A., Dieux, A., Afenjar, A., Ghoumid, J., Diebold, B., Mietton, L., Briand-Suleau, A., Billuart, P., and Bienvenu, T. (2018). Molecular and cellular issues of KMT2A variants involved in Wiedemann-Steiner syndrome. Eur. J. Hum. Genet. *26*, 107–116.
40. Tatton-Brown, K., Seal, S., Ruark, E., Harmer, J., Ramsay, E., Del Vecchio Duarte, S., Zachariou, A., Hanks, S., O'Brien, E., Aksglaede, L., et al.; Childhood Overgrowth Consortium (2014). Mutations in the DNA methyltransferase gene DNMT3A cause an overgrowth syndrome with intellectual disability. Nat. Genet. *46*, 385–388.
41. Davarniya, B., Hu, H., Kahrizi, K., Musante, L., Fattahi, Z., Hosseini, M., Maqsoud, F., Farajollahi, R., Wienker, T.F., Ropers, H.H., and Najmabadi, H. (2015). The Role of a Novel TRMT1 Gene Mutation and Rare GRM1 Gene Defect in Intellectual Disability in Two Azeri Families. PLoS ONE *10*, e0129631.
42. Khan, M.A., Rafiq, M.A., Noor, A., Hussain, S., Flores, J.V., Rupp, V., Vincent, A.K., Malli, R., Ali, G., Khan, F.S., et al. (2012). Mutation in NSUN2, which encodes an RNA methyltransferase, causes autosomal-recessive intellectual disability. Am. J. Hum. Genet. *90*, 856–863.
43. Abbasi-Moheb, L., Mertel, S., Gonsior, M., Nouri-Vahid, L., Kahrizi, K., Cirak, S., Wieczorek, D., Motazacker, M.M., Esmaeeli-Nieh, S., Cremer, K., et al. (2012). Mutations in NSUN2 cause autosomal-recessive intellectual disability. Am. J. Hum. Genet. *90*, 847–855.
44. Freude, K., Hoffmann, K., Jensen, L.R., Delatycki, M.B., des Portes, V., Moser, B., Hamel, B., van Bokhoven, H., Moraine, C., Fryns, J.P., et al. (2004). Mutations in the FTSJ1 gene coding for a novel S-adenosylmethionine-binding protein cause nonsyndromic X-linked mental retardation. Am. J. Hum. Genet. *75*, 305–309.
45. Kleefstra, T., Schenck, A., Kramer, J.M., and van Bokhoven, H. (2014). The genetics of cognitive epigenetics. Neuropharmacology *80*, 83–94.
46. Iwase, S., Bérubé, N.G., Zhou, Z., Kasri, N.N., Battaglioli, E., Scandaglia, M., and Barco, A. (2017). Epigenetic Etiology of Intellectual Disability. J. Neurosci. *37*, 10773–10782.
47. Franke, C., Gräfe, D., Bartsch, H., and Bachmann, M.P. (2015). Use of Nonradioactive Detection Method for North- and South-Western Blot. Methods Mol. Biol. *1314*, 63–71.
48. Parashar, N.C., Parashar, G., Nayyar, H., and Sandhir, R. (2018). N^6-adenine DNA methylation demystified in eukaryotic genome: From biology to pathology. Biochimie *144*, 56–62.
49. Yao, B., Cheng, Y., Wang, Z., Li, Y., Chen, L., Huang, L., Zhang, W., Chen, D., Wu, H., Tang, B., and Jin, P. (2017). DNA N6-methyladenine is dynamically regulated in the mouse brain following environmental stress. Nat. Commun. *8*, 1122.
50. Lesbirel, S., and Wilson, S.A. (2019). The m^6A-methylase complex and mRNA export. Biochim. Biophys. Acta. Gene Regul. Mech. *1862*, 319–328.
51. Meyer, K.D. (2019). m^6A-mediated translation regulation. Biochim. Biophys. Acta. Gene Regul. Mech. *1862*, 301–309.
52. Malla, S., Melguizo-Sanchis, D., and Aguilo, F. (2019). Steering pluripotency and differentiation with N^6-methyladenosine RNA modification. Biochim. Biophys. Acta. Gene Regul. Mech. *1862*, 394–402.
53. Liu, J., Yue, Y., Han, D., Wang, X., Fu, Y., Zhang, L., Jia, G., Yu, M., Lu, Z., Deng, X., et al. (2014). A METTL3-METTL14 complex mediates mammalian nuclear RNA N6-adenosine methylation. Nat. Chem. Biol. *10*, 93–95.
54. Wang, Y., Li, Y., Yue, M., Wang, J., Kumar, S., Wechsler-Reya, R.J., Zhang, Z., Ogawa, Y., Kellis, M., Duester, G., and Zhao, J.C. (2018). N^6-methyladenosine RNA modification regulates

embryonic neural stem cell self-renewal through histone modifications. Nat. Neurosci. *21*, 195–206.

55. Wang, C.X., Cui, G.S., Liu, X., Xu, K., Wang, M., Zhang, X.X., Jiang, L.Y., Li, A., Yang, Y., Lai, W.Y., et al. (2018). METTL3-mediated m6A modification is required for cerebellar development. PLoS Biol. *16*, e2004880.
56. Koranda, J.L., Dore, L., Shi, H., Patel, M.J., Vaasjo, L.O., Rao, M.N., Chen, K., Lu, Z., Yi, Y., Chi, W., et al. (2018). Mettl14 Is Essential for Epitranscriptomic Regulation of Striatal Function and Learning. Neuron *99*, 283–292.e5.
57. Zhang, Z., Wang, M., Xie, D., Huang, Z., Zhang, L., Yang, Y., Ma, D., Li, W., Zhou, Q., Yang, Y.G., and Wang, X.J. (2018). METTL3-mediated N^6-methyladenosine mRNA modification enhances long-term memory consolidation. Cell Res. *28*, 1050–1061.
58. Warda, A.S., Kretschmer, J., Hackert, P., Lenz, C., Urlaub, H., Höbartner, C., Sloan, K.E., and Bohnsack, M.T. (2017). Human METTL16 is a N^6-methyladenosine (m^6A) methyltransferase that targets pre-mRNAs and various non-coding RNAs. EMBO Rep. *18*, 2004–2014.

The American Journal of Human Genetics, Volume *105*

Supplemental Data

Bi-allelic Variants in *METTL5* Cause Autosomal-Recessive Intellectual Disability and Microcephaly

Elodie M. Richard, Daniel L. Polla, Muhammad Zaman Assir, Minerva Contreras, Mohsin Shahzad, Asma A. Khan, Attia Razzaq, Javed Akram, Moazzam N. Tarar, Thomas A. Blanpied, Zubair M. Ahmed, Rami Abou Jamra, Dagmar Wieczorek, Hans van Bokhoven, Sheikh Riazuddin, and Saima Riazuddin

Supplemental note:

Case reports

For family PKMR43M, both parents of affected individuals have been interviewed to obtain information on prenatal, perinatal, and neonatal medical history and developmental milestones. A detailed history of neurological and systemic symptoms was obtained and functional capacity including self-care, education, special needs and social interaction was documented. Physical examination of all affected and unaffected children included documenting of motor milestones, weight, height, head circumference, morphological abnormality screening, musculoskeletal features, deep tendon reflexes, gait, cerebellar functions, and verbal and motor aptitude. Furthermore, all affected individuals have been clinically evaluated for any ophthalmological, audiological, vestibular, or dermatological abnormalities. ID severity has been classified as severe based on measures of developmental milestones /criteria from American Association on Intellectual & Developmental Disability.

In addition to phenotypic features presented in the main text, all three affected individuals of PKMR43 had considerable delay (months to years) in childhood development milestones in all domains including cognitive development, social and emotional development, speech and language development, and gross motor and fine motor skill development. At the time of evaluation, all three individuals could understand speech but were unable to communicate. They could eat and drink but needed significant supervision for execution of other activities of daily living. All individuals had aggressive behavior. They could not travel alone. Brain MRI were acquired after the first evaluation of the family, based on the microcephaly of the affected individuals.

For family F47949, we had interviews with the parents and physical examinations of the brothers in our department as described above. No formal IQ testing was performed. ID severity has been classified as severe based on criteria described in Zhang et al [1]. Patient III:2 has an IQ between 20 and 35 (moderate to severe) and patient III:3 has an IQ between 10 and 20 (severe). The elder brothers learned walking without support at the age of 3 years and was able to talk simple sentences at the age of 9 years. He was not able to write, read or calculate. The younger brother learned walking at the age of 3,5 years, he did not speak any word at the age of nearly 5 years. Both brothers were biting their hands.

For family from Hu et al (2019), HAWIK-IV showed IQs of 25 and 26 for patients III:3 and III:5, respectively [2].

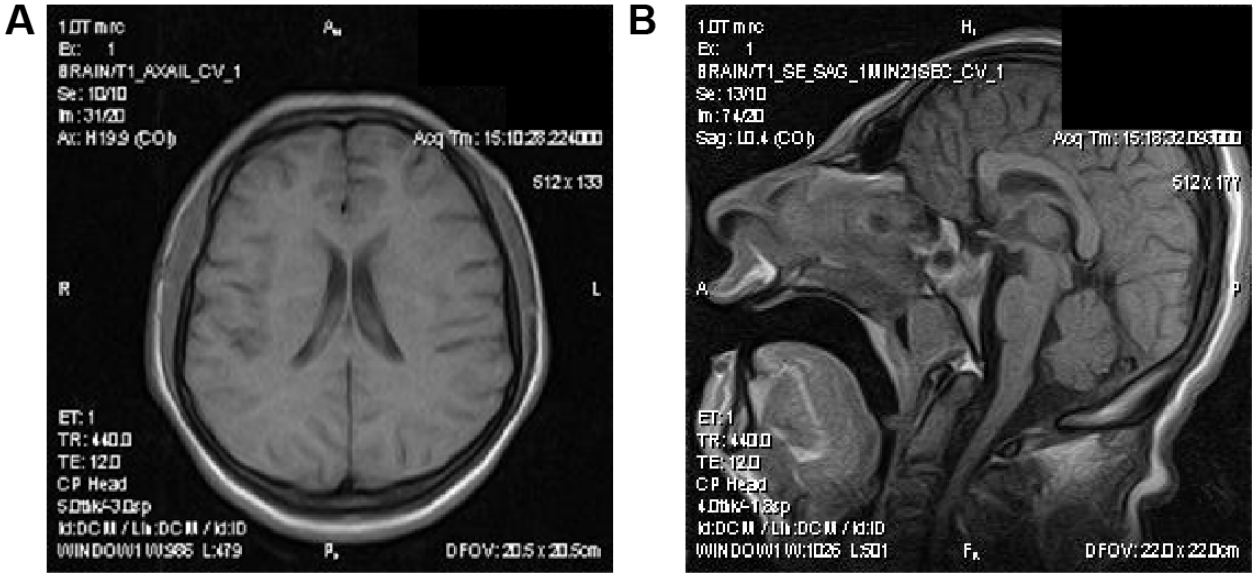

Figure S1. MRI of individual PKMR43M II-2 confirms microcephaly.

(A) MRI of an axial section of individual PKMR43M II-2 brain while (B) MRI of a sagittal section confirms microcephaly.

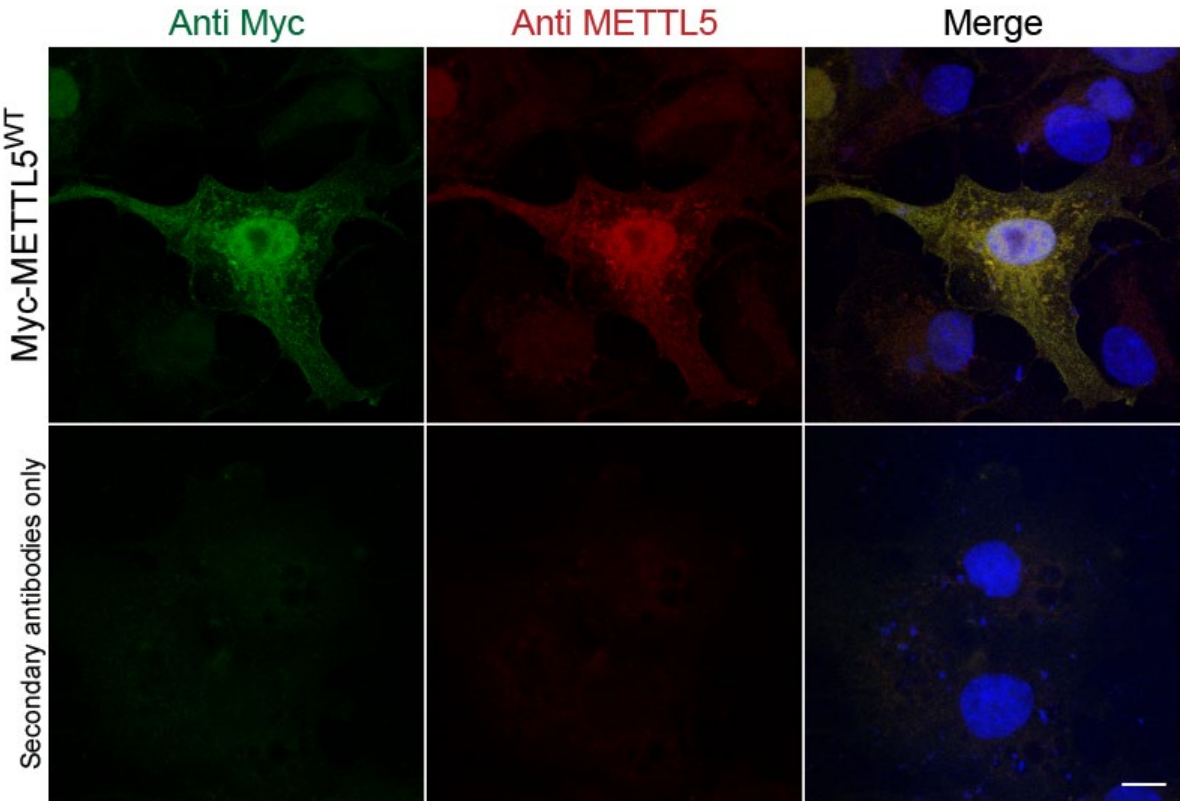

Figure S2. Validation of METTL5 (Novus Biologicals) antibody.

To validate the METTL5 antibody, COS7 cells were transiently transfected with Myc-METTL5 cDNA construct. After 48h, the cells were fixed, permeabilized and immunolabeled with a Myc antibody (Covance Research Products Inc Cat# MMS-164P-100, RRID:AB_291335) and METTL5 antibody (Novus Biologicals Cat# NBP1-56640, RRID:AB_11039697). The nuclei were counterstained with DAPI (blue). Myc staining (green) and METTL5 staining (red) colocalize (merge) showing that METTL5 antibody can recognize the transfected protein. The bottom panel represent cells that were submitted to the same immunolabeling protocol with the exception of the incubation with the primary antibodies, namely Myc and METTL5. No signal was detected in this specific case. All images are projection of confocal optical sections stack. Scale bar: 10µm.

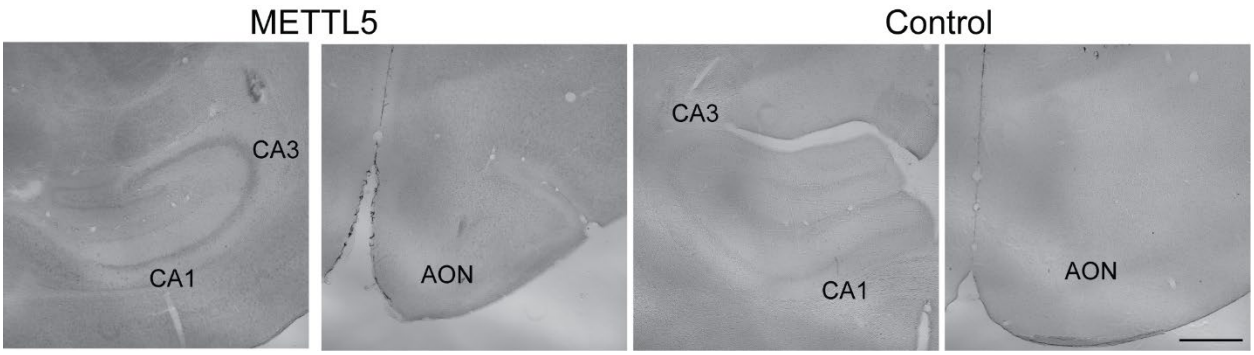

Figure S3. Immunolocalization of Mettl5 in the mouse brain.

Immunolocalization of Mettl5 in P30 mouse brain, using a 3,3′-Diaminobenzidine (DAB) based immunochemistry procedure, shows a faint and diffuse staining in different structures, absent in the control slices (no primary antibody). CA1 and CA3 of the hippocampus, AON: anterior olfactory nucleus. Scale bar: 500μm.

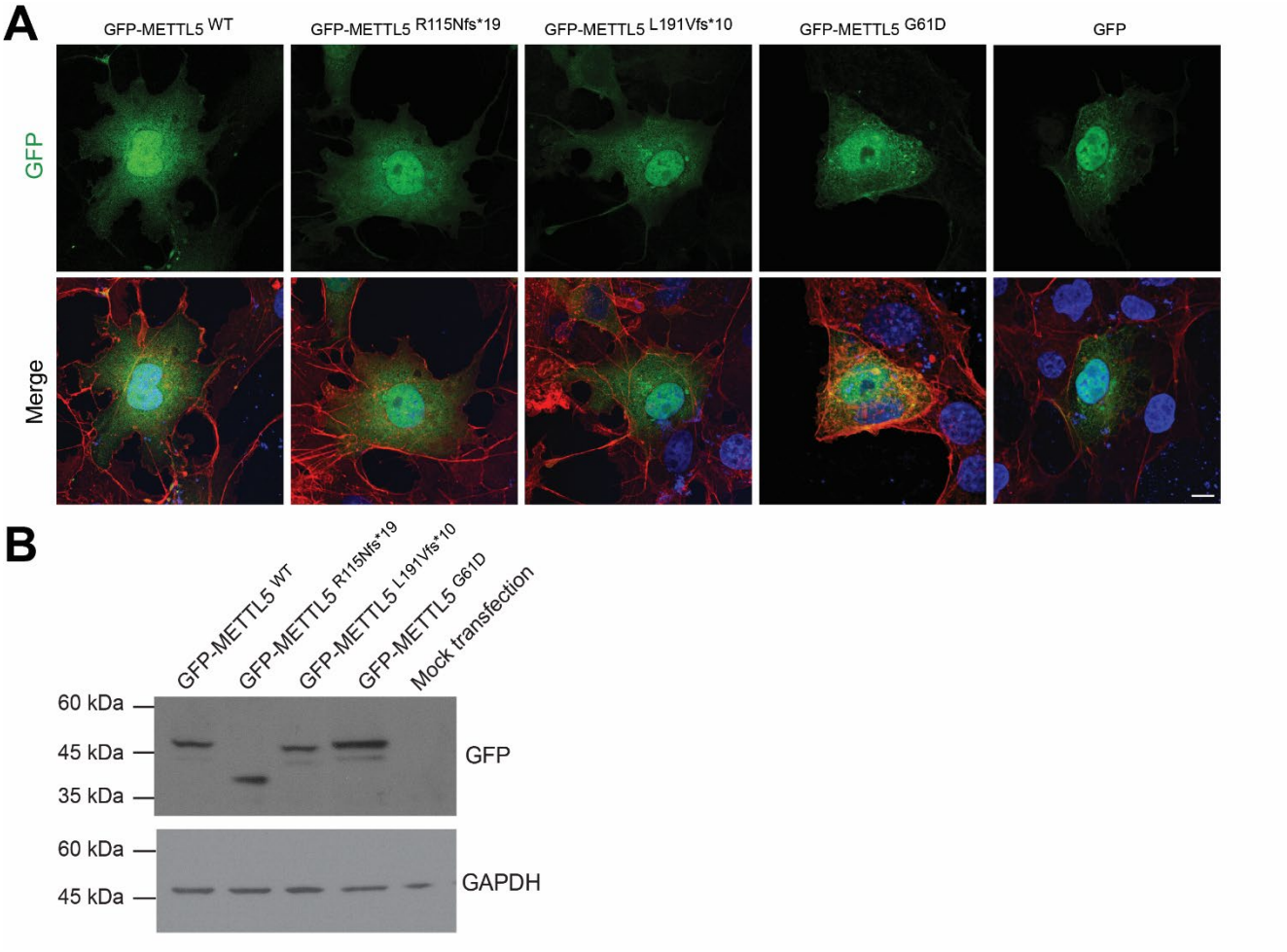

Figure S4. Steady state level and localization of GFP-METTL5.

To validate the results obtained with Myc-METTL5, we performed localization in transfected COS7 cells and Western Blot analysis on transfected HEK cells with GFP-METTL5 constructs. (A) GFP-METTL5 fusion proteins for WT and the 3 variants associated with ID, after transfection in COS7 cells. The subcellular localization shows that, like Myc-METTL5 proteins, GFP-METTL5 WT and the three disease-associated mutant proteins (green) accumulate in the nucleus (blue) and forms aggregates in the cytoplasm. All images are projection of confocal optical sections stack. Scale bar: 10µm. (B) Western Blot on transfected HEK293T cells with GFP-METTL5 WT or mutant constructs, using GFP antibodies (Molecular Probes Cat# A-11122, RRID:AB_221569) did not reveal any decrease of the steady state level of the mutant proteins. We hypothesized that the GFP tag, due to its large size (27kDa), is conferring stability to the synthesized mutant proteins METTL5 ^{R115Nfs*19} and METTL5^{L191Vfs*10} (15kDa and 23kDa respectively). GAPDH (Santa Cruz Biotechnology Cat# sc-32233, RRID:AB_627679) was used as loading control.

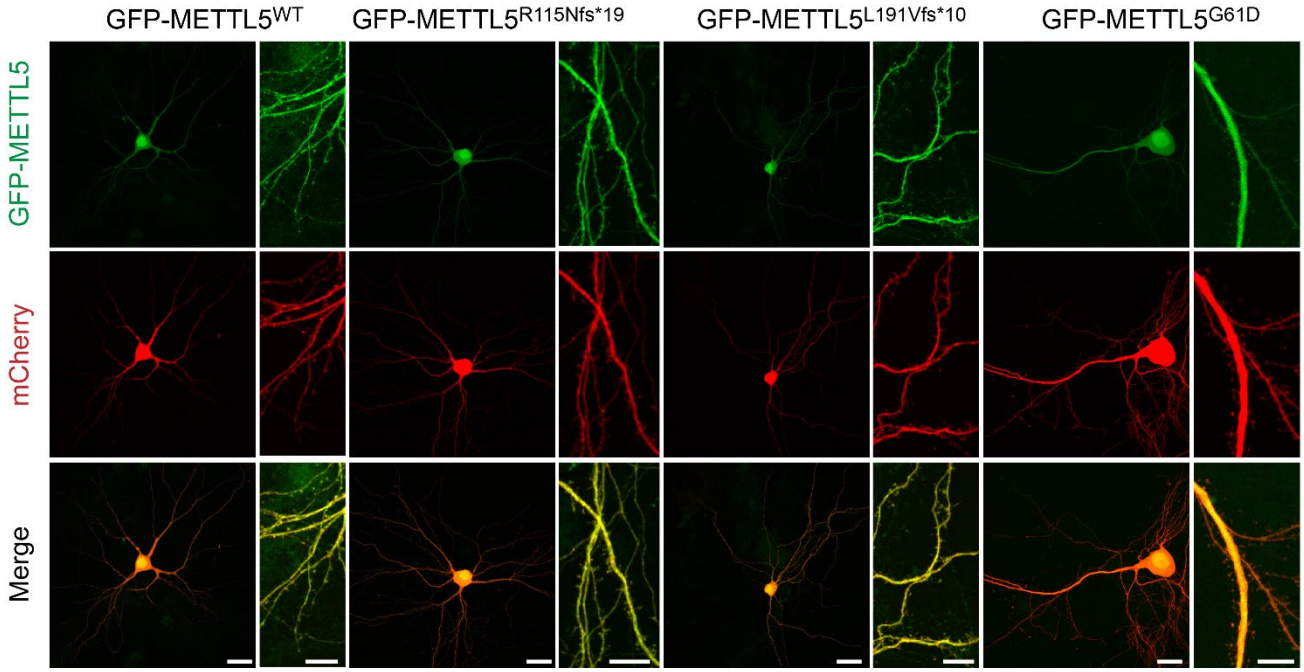

Figure S5. METTL5 variants do not affect the synapse morphology.

Transfected rat hippocampal neurons with GFP-METTL5 fusion proteins for WT and the three disease-causing variants (green) constructs and pmCherry-N1 vector (Takara, red). None of the variant affect the morphology of the dendrites nor localization of the protein in transfected neurons. All images are projection of confocal optical sections stack. Scale bars: 24 and 10μm.

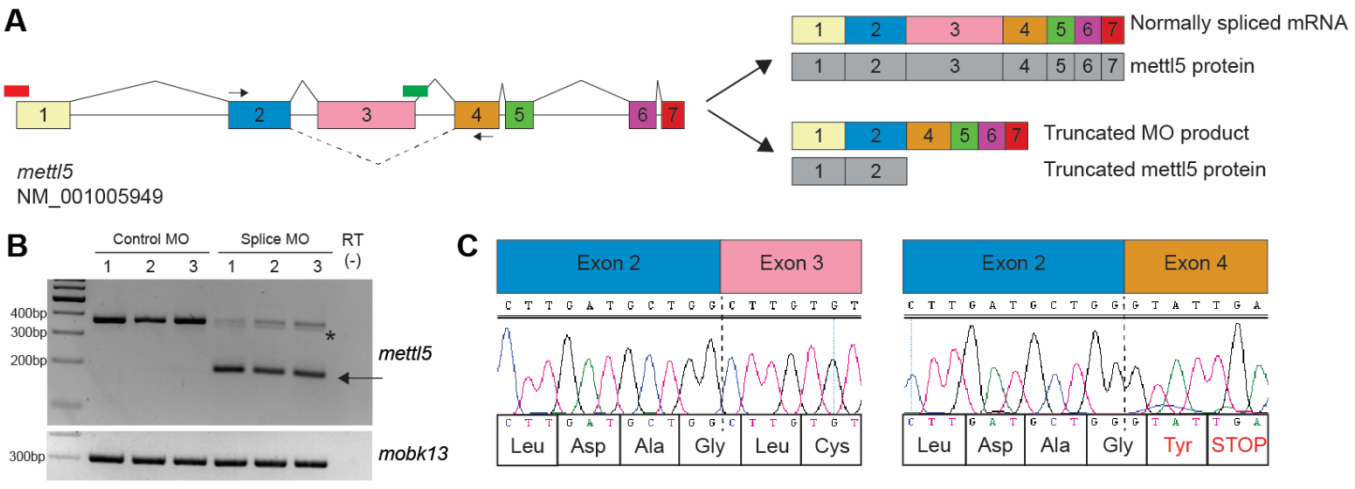

Figure S6. Anti-sense *mettl5* morpholino retains intron 4 and leads to a truncated protein. (A) Schematic diagram of the zebrafish *mettl5* gene, showing: exons (numbered blocks); ATG MO and splice MO targets (red and green blocks, respectively); PCR primers flanking exon 3 (black arrows, sequences are available upon request). (B) Knockdown in splice-targeting MO injected embryos was verified using RT-PCR. Embryos were injected with a Control MO (5ng) or *mettl5* splice-targeting MO (5ng). Arrow indicates the alternative splice products induced by *mettl5* splice-targeting MO injection. An additional band, indicated by an asterisk (*), was produced due to the activation of a cryptic splice site in exon 3. (C) Sanger sequencing of PCR products confirmed that injection of *mettl5* splice-targeting MO results in the absence of exon 3. A novel, in-frame, pre-mature stop codon was generated in exon 4.

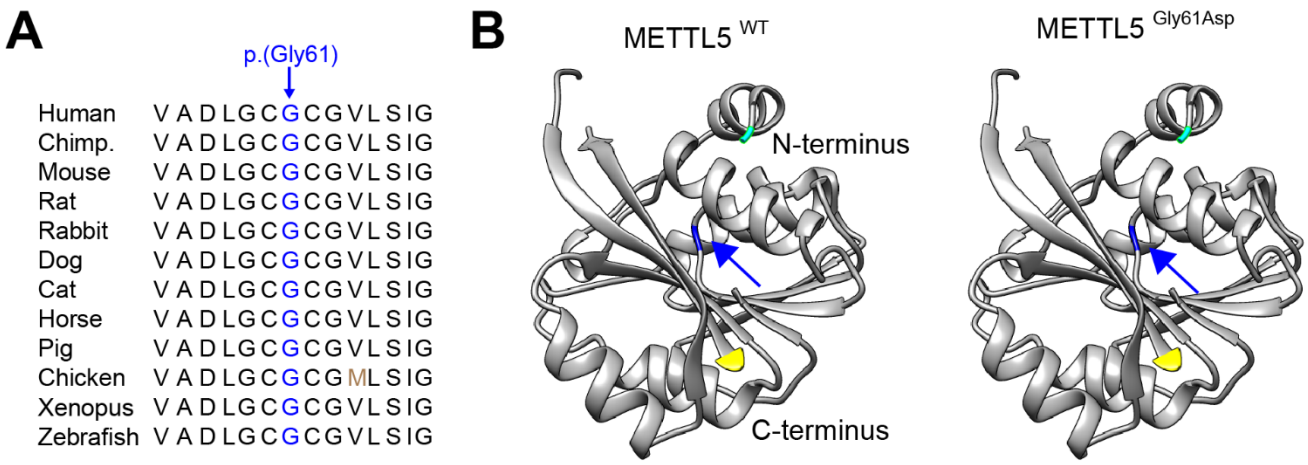

Figure S7. METTL5 p.(G61) is highly conserved among species but p.(G61D) variant does not affect the conformation of the mutant protein.
(A) The glycine residue at amino-acid position 61, depicted in blue, is completely conserved across a wide variety of species. (B) Protein modeling of the WT and METTL5^{G61D} proteins, using PHYRE2 software [3] shows that the overall conformation of the protein is not affected.

Table S2: Classification of the candidate variants based on ACMG guidelines

	Classification	**ACMG criteria used [4]**
c.182G>A; p.(Gly61Asp)	Variant of uncertain significance	PM2, PP1, PP3
c.344_345delGA; p.(Arg115Asnfs*19)	Pathogenic	PS3, PM2, PM4, PP1, PP3
c.571_572delAA; p.(Lys191Valfs*10)	Pathogenic	PS3, PM2, PM4, PP1, PP3

Table S3: Pathogenicity prediction results for *METTL5* variant [c.182G>A; p.(Gly61Asp)]

c.DNA variant	Protein variant	Polyphen-2(1)		PROVEAN (2) (score)	SIFT (3) (score)	Mutation Taster(4) (score)	gnomAD(5) frequency	ExAC(6) frequency	CADD(7) score
		HUM-DIV (score)	HUM-VAR (score)						
c.182G>A	p.(Gly61Asp)	Probably damaging (1)	Probably damaging (1)	Deleterious (-7)	Damaging (0)	Disease causing (0.999)	NA	NA	26

(1) Polyphen-2, http://genetics.bwh.harvard.edu/pph2, cut-off: <0.15 (possibly damaging) [5]
(2) PROVEAN, http://provean.jcvi.org/genome_submit_2.php?species=human, cut-off: <-2.5 (damaging) [6; 7]
(3) SIFT (from PROVEAN), http://provean.jcvi.org/genome_submit_2.php?species=human, cut-off: <0.05 (damaging) [8]
(4) MutationTaster, http://www.mutationtaster.org/, cut-off: 1 = high confidence of prediction
(5) gnomAD, genome Aggregation Database, https://gnomad.broadinstitute.org [9]
(6) ExAC, Exome Aggregation Consortium , http://exac.broadinstitute.org [9]
(7) CADD, Combined Annotation Dependent Depletion, https://cadd.gs.washington.edu [10; 11]

Supplemental References

1. Zhang, X., Snijders, A., Segraves, R., Zhang, X., Niebuhr, A., Albertson, D., Yang, H., Gray, J., Niebuhr, E., Bolund, L., et al. (2005). High-resolution mapping of genotype-phenotype relationships in cri du chat syndrome using array comparative genomic hybridization. Am J Hum Genet 76, 312-326.
2. Hu, H., Kahrizi, K., Musante, L., Fattahi, Z., Herwig, R., Hosseini, M., Oppitz, C., Abedini, S.S., Suckow, V., Larti, F., et al. (2018). Genetics of intellectual disability in consanguineous families. Mol Psychiatry 24, 1027-1039.
3. Kelley, L.A., Mezulis, S., Yates, C.M., Wass, M.N., and Sternberg, M.J. (2015). The Phyre2 web portal for protein modeling, prediction and analysis. Nat Protoc 10, 845-858.
4. Richards, S., Aziz, N., Bale, S., Bick, D., Das, S., Gastier-Foster, J., Grody, W.W., Hegde, M., Lyon, E., Spector, E., et al. (2015). Standards and guidelines for the interpretation of sequence variants: a joint consensus recommendation of the American College of Medical Genetics and Genomics and the Association for Molecular Pathology. Genet Med 17, 405-424.
5. Adzhubei, I., Jordan, D.M., and Sunyaev, S.R. (2013). Predicting functional effect of human missense mutations using PolyPhen-2. Curr Protoc Hum Genet Chapter 7, Unit7 20.
6. Choi, Y., Sims, G.E., Murphy, S., Miller, J.R., and Chan, A.P. (2012). Predicting the functional effect of amino acid substitutions and indels. PLoS One 7, e46688.
7. Choi, Y., and Chan, A.P. (2015). PROVEAN web server: a tool to predict the functional effect of amino acid substitutions and indels. Bioinformatics 31, 2745-2747.
8. Sim, N.L., Kumar, P., Hu, J., Henikoff, S., Schneider, G., and Ng, P.C. (2012). SIFT web server: predicting effects of amino acid substitutions on proteins. Nucleic Acids Res 40, W452-457.
9. Lek, M., Karczewski, K.J., Minikel, E.V., Samocha, K.E., Banks, E., Fennell, T., O'Donnell-Luria, A.H., Ware, J.S., Hill, A.J., Cummings, B.B., et al. (2016). Analysis of protein-coding genetic variation in 60,706 humans. Nature 536, 285-291.
10. Kircher, M., Witten, D.M., Jain, P., O'Roak, B.J., Cooper, G.M., and Shendure, J. (2014). A general framework for estimating the relative pathogenicity of human genetic variants. Nat Genet 46, 310-315.
11. Rentzsch, P., Witten, D., Cooper, G.M., Shendure, J., and Kircher, M. (2019). CADD: predicting the deleteriousness of variants throughout the human genome. Nucleic Acids Res 47, D886-D894.